Torque Saturation in Bipedal Robotic Walking Through Control Lyapunov Function-Based Quadratic Programs

KEVIN GALLOWAY[1], KOUSHIL SREENATH[2], AARON D. AMES[3], AND JESSY W. GRIZZLE[4], (Fellow, IEEE)

[1]Department of Electrical and Computer Engineering, United States Naval Academy, Annapolis, MD 21401, USA
[2]Department of Mechanical Engineering, the Department of Electrical and Computer Engineering, Robotics Institute, Carnegie Mellon University, Pittsburgh, PA 15213, USA
[3]Department of Mechanical Engineering, Texas A&M University, College Station, TX 77843, USA
[4]Control Systems Laboratory, Department of Electrical Engineering and Computer Science, University of Michigan, Ann Arbor, MI 48109, USA

Corresponding author: K. Galloway (kgallowa@usna.edu)

ABSTRACT This paper presents a novel method to address the actuator saturation for nonlinear hybrid systems by directly incorporating user-defined input bounds in a controller design. In particular, we consider the application of bipedal walking and show that our method [based on a quadratic programming (QP) implementation of a control Lyapunov function (CLF)-based controller] enables a gradual performance degradation while still continuing to walk under increasingly stringent input bounds. We draw on our previous work, which has demonstrated the effectiveness of the CLF-based controllers for stabilizing periodic gaits for biped walkers. This paper presents a framework, which results in more effective handling of control saturations and provides a means for incorporating a whole family of user-defined constraints into the online computation of a CLF-based controller. This paper concludes with an experimental validation of the main results on the bipedal robot MABEL, demonstrating the usefulness of the QP-based CLF approach for real-time robotic control.

INDEX TERMS Quadratic programming, legged locomotion, Lyapunov methods.

I. INTRODUCTION

Biped locomotion presents an interesting control challenge, especially since the dynamic models are typically hybrid and underactuated. The method of Hybrid Zero Dynamics (HZD) [2], [3] has provided a rigorous and intuitive method for implementing periodic walking gaits in such robotic systems, by driving the system to a lower-dimensional zero dynamics manifold on which the walking gait exists as an exponentially stable periodic orbit. Typical experimental implementation of the HZD method has relied on input-output linearization with PD control to drive the system to the zero dynamics manifold [4], but recent work by the authors has demonstrated that control Lyapunov function (CLF)-based controllers can be used to effectively implement stable walking, both in simulation and in experimental contexts [1].

A variant formulation known as an exponentially stabilizing control Lyapunov function (ES-CLF) provides a means for not only guaranteeing exponential stability of a system but also providing an explicit bound on the rate of convergence. In the case of hybrid systems (such as biped robots with impulsive foot-ground impact), an even stronger convergence property is required, and therefore we turn to rapidly exponentially stabilizing control Lyapunov functions (RES-CLF).[1] This type of CLF, which will be reviewed in more detail in Section II, incorporates an additional tuning parameter which allows the user to directly control the rate of exponential convergence. The work in [1] established the key theoretical properties of CLF-based controllers in a hybrid context, and also presented a description of the successful experimental implementation of a CLF-based controller on the robotic testbed MABEL. However, it was also noted that the user-defined

---

[1]This stronger convergence property is required to meet the conditions described in [1, Th. 2], which relates stability of a hybrid periodic orbit in the zero manifold to stability of the orbit in the full space.

control saturations were active throughout a large portion of the walking experiment, and that these saturations had a significant impact on the actual performance of the CLF-based controller as compared to the predicted performance based on theoretical bounds. In this context the hard torque limits were "blindly" applied to the calculated CLF-based control torques, without explicit consideration of the potential effect on the controller performance.

The impact of actuator saturation in feedback systems is often detrimental to stability and performance, and it therefore has been the study of a large body of research. (See [5] for instance, which provides an extensive bibliography on the topic.) In the context of robotic biped locomotion, torque saturations can limit the ability to recover from disturbances and result in instability. Typically, torque saturation is considered during the design of walking gaits, where actuator limitations are included as inequality constraints for an offline gait-design optimization routine (see [6] for instance). However, while this approach can guarantee that the torques required on the periodic walking gait are within limits, it does not account for disturbances such as rough terrain or model uncertainties which demand higher torques during recovery phase. In other work, such as [7], an optimal decision strategy in the form of an optimal control problem is solved point-wise in time to minimize the deviation between the joint accelerations and the desired joint accelerations subject to input constraints. The authors also extend this to handle robustness when the plant model is not known precisely. Further, in [8], torque saturations are incorporated into calculation of a feedback control designed to track a time-based reference trajectory, with tracking error traded off in order to keep torque controls within limits.

The main contribution of this paper is to provide a novel control design framework for application to bipedal robotics that enables gradual performance degradation while still continuing to walk under a range of stringent torque limits. We achieve this through an alternative method of controller implementation based on quadratic programming (QP), that not only preserves (as much as possible) the desirable performance characteristics promised by the CLF theory, but also respects the user-defined bounds on the inputs. Recent work in [9] has shown that QP implementation of CLF-based policies can be made feasible for real-time implementation with standard processor speeds. However, this work focuses on linear time-varying systems, and not the nonlinear hybrid systems we consider. The use of QP can also be found in biped control applications, as in [10] for realizing desired link accelerations, in [11] for maintaining balance after disturbances by modifying predefined reference trajectories, and in [12] and [13] for applying model predictive control approaches to biped control. The main contribution of the current work is to use QP to obtain RES-CLF convergence properties (to the extent possible) for a nonlinear hybrid system in the face of input constraints, and demonstrate the practicality of the approach through a non-trivial experimental implementation on a biped robot.

The paper proceeds as follows. In Section II, we state the dynamics of the relevant model and review the results on CLF-based control of biped robots from [1]. Section III discusses the adverse effects of user-specified control input saturations on the CLF-based controller, providing the motivation for Section IV which introduces a new method for using quadratic programming to appropriately handle torque saturation constraints for the CLF-based controllers. Section V presents simulation and experimental results, and we conclude with a summary in Section VI.

II. CONTROL LYAPUNOV FUNCTIONS FOR HYBRID SYSTEMS REVISITED

In this section we introduce the model for a biped robot and review the recent innovations introduced in [1] for using control Lyapunov functions to control such systems.

A. MODEL

The dynamics for a biped robot (such as MABEL, the robot described in Section V) can be derived by the standard method of Lagrange and take the form

$$D(q)\ddot{q} + C(q, \dot{q})\dot{q} + G(q) = B(q)u, \qquad (1)$$

where $q \in \mathcal{Q}$ is the robot configuration variable, u represents the motor control torques, and D, C and G are respectively the inertia matrix, Coriolis matrix, and gravity vector. In the case of MABEL the configuration vector q is 7-dimensional and is as described in [4] and depicted in Figure 7a, while u is 4-dimensional. Reformulating the dynamics (1) as

$$\begin{bmatrix} \dot{q} \\ \ddot{q} \end{bmatrix} = f(q, \dot{q}) + g(q, \dot{q})u, \qquad (2)$$

we also define output functions of the form $y(q)$.[2] The method of Hybrid Zero Dynamics (HZD) aims to drive these output functions (and their first derivatives) to zero, thereby imposing "virtual constraints" such that the system evolves on the lower-dimensional zero dynamics manifold, given by

$$Z = \{(q, \dot{q}) \in T\mathcal{Q} \mid y(q) = 0, \ L_f y(q, \dot{q}) = 0\}, \qquad (3)$$

where L_f denotes the Lie derivative [14].

Bipedal walking has unilateral ground contact constraints as well as friction cone constraints at the stance leg. We address this in the design of our nominal walking gait through a nonlinear constrained optimization process that explicitly respects the unilateral contact force as well as the friction cone constraints.

B. INPUT-OUTPUT LINEARIZATION

If $y(q)$ has vector relative degree 2, then the second derivative takes the form

$$\ddot{y} = L_f^2 y(q, \dot{q}) + L_g L_f y(q, \dot{q})u, \qquad (4)$$

---

[2]More specifically, the output functions take the form $y(q) := H_0 q - y_d(\theta(q))$, where $\theta(q)$ is a strictly monotonic function of the configuration variable q, H_0 is an appropriately-sized matrix prescribing linear combinations of state variables to be controlled, and $y_d(\cdot)$ prescribes the desired evolution of these quantities. (See [4] for details.)

where the decoupling matrix $L_g L_f y(q, \dot{q})$ is invertible due to the vector relative degree assumption. Then defining

$$u^*(q, \dot{q}) := -(L_g L_f y(q, \dot{q}))^{-1} L_f^2 y(q, \dot{q}), \quad (5)$$

and applying a pre-control law of the form

$$u(q, \dot{q}) = u^*(q, \dot{q}) + \mu \quad (6)$$

or

$$u(q, \dot{q}) = u^*(q, \dot{q}) + (L_g L_f y(q, \dot{q}))^{-1} \mu \quad (7)$$

renders Z invariant (provided μ vanishes on Z). (Note that $u^*(q, \dot{q})$ is a feed-forward term representing the torque required to remain on Z.)

Under these assumptions, the dynamics (2) can be decomposed into zero dynamics states $z \in Z$ and transverse variables $\eta = \begin{bmatrix} y \\ \dot{y} \end{bmatrix}$. (See [3], [14] for details.) Under a pre-control law of the form (6) or (7), the closed-loop dynamics in terms of (η, z) take the form

$$\dot{\eta} = \bar{f}(\eta, z) + \bar{g}(\eta, z)\mu \quad (8)$$
$$\dot{z} = f_z(\eta, z). \quad (9)$$

For the work presented here, we will use the pre-control law (7) so that $\bar{f}(\eta, z) = F\eta$ and $\bar{g}(\eta, z) = G$, where

$$F = \begin{bmatrix} 0 & I \\ 0 & 0 \end{bmatrix}, \quad G = \begin{bmatrix} 0 \\ I \end{bmatrix}. \quad (10)$$

The most common approach to controlling the transverse variables (i.e. driving η to zero) relies on input-output linearization with PD control, using (7) with

$$\mu = \begin{bmatrix} -\frac{1}{\varepsilon^2} K_P & -\frac{1}{\varepsilon} K_D \end{bmatrix} \eta, \quad (11)$$

where K_P and K_D are diagonal matrices chosen such that the matrix

$$\begin{bmatrix} 0 & I \\ -K_P & -K_D \end{bmatrix} \quad (12)$$

is Hurwitz.

C. CLF-BASED CONTROL

Recently, a new method based on control Lyapunov functions has been introduced in [1], which provides an alternative method for controlling the transverse variables. That method can be summarized as follows.

A function $V_\varepsilon(\eta)$ is a *rapidly exponentially stabilizing control Lyapunov function (RES-CLF)* for the system (8)-(9) if there exist strictly positive constants c_1, c_2, c_3 such that for all $0 < \varepsilon < 1$ and all states (η, z) it holds that

$$c_1 \|\eta\|^2 \leq V_\varepsilon(\eta) \leq \frac{c_2}{\varepsilon^2} \|\eta\|^2 \quad (13)$$

$$\inf_{\mu \in U} \left[L_{\bar{f}} V_\varepsilon(\eta, z) + L_{\bar{g}} V_\varepsilon(\eta, z)\mu + \frac{c_3}{\varepsilon} V_\varepsilon(\eta) \right] \leq 0, \quad (14)$$

where U is the set of all possible controls. One way to generate a RES-CLF $V_\varepsilon(\eta)$ is to first solve the Lyapunov equation $A^T P + PA = -Q$ for P (where A is the matrix given

in (12) and Q is any symmetric positive-definite matrix), and then define

$$V_\varepsilon(\eta) = \eta^T \begin{bmatrix} \frac{1}{\varepsilon}I & 0 \\ 0 & I \end{bmatrix} P \begin{bmatrix} \frac{1}{\varepsilon}I & 0 \\ 0 & I \end{bmatrix} \eta =: \eta^T P_\varepsilon \eta, \quad (15)$$

for which we have

$$L_{\bar{f}} V_\varepsilon(\eta, z) = \eta^T (F^T P_\varepsilon + P_\varepsilon F)\eta,$$
$$L_{\bar{g}} V_\varepsilon(\eta, z) = 2\eta^T P_\varepsilon G. \quad (16)$$

Associated with a RES-CLF is the set of all μ for which (14) is satisfied,

$$K_\varepsilon(\eta, z) = \{ \mu \in U : L_{\bar{f}} V_\varepsilon(\eta, z) + L_{\bar{g}} V_\varepsilon(\eta, z)\mu$$
$$+ \frac{c_3}{\varepsilon} V_\varepsilon(\eta) \leq 0 \},$$

and one can show that for any Lipschitz continuous feedback control law $\mu_\varepsilon(\eta, z) \in K_\varepsilon(\eta, z)$, it holds that

$$\|\eta(t)\| \leq \frac{1}{\varepsilon} \sqrt{\frac{c_2}{c_1}} e^{-\frac{c_3}{2\varepsilon}t} \|\eta(0)\|, \quad (17)$$

i.e., the rate of exponential convergence to the zero dynamics manifold can be directly controlled with the constant ε through $\frac{c_3}{\varepsilon}$. There are various methods for finding a feedback control law $\mu_\varepsilon(\eta, z) \in K_\varepsilon(\eta, z)$; in practical applications, it is often important to select the control law of minimum norm. If we let $c_3 = \frac{\lambda_{\min}(Q)}{\lambda_{\max}(P)}$ (where $\lambda_{\min}$ and $\lambda_{\max}$ denote the minimum and maximum eigenvalues of a matrix, respectively) and define

$$\psi_{0,\varepsilon}(\eta, z) = L_{\bar{f}} V_\varepsilon(\eta, z) + \frac{c_3}{\varepsilon} V_\varepsilon(\eta, z)$$
$$\psi_{1,\varepsilon}(\eta, z) = L_{\bar{g}} V_\varepsilon(\eta, z)^T, \quad (18)$$

then this pointwise min-norm control law [15] can be explicitly formulated as

$$\mu_\varepsilon(\eta, z) = \begin{cases} -\dfrac{\psi_{0,\varepsilon}(\eta, z)\psi_{1,\varepsilon}(\eta, z)}{\psi_{1,\varepsilon}(\eta, z)^T \psi_{1,\varepsilon}(\eta, z)} & \text{if } \psi_{0,\varepsilon}(\eta, z) > 0 \\ 0 & \text{if } \psi_{0,\varepsilon}(\eta, z) \leq 0, \end{cases} \quad (19)$$

wherein we can take $\mu = \mu_\varepsilon$ in (7).

III. ADVERSE EFFECTS OF TORQUE SATURATION ON THE CLF-BASED CONTROLLER

The approach described in Section II was successfully implemented on the robotic testbed MABEL, producing a stable walking gait.[3] However, analysis of the experimental data reveals that the user-imposed saturations on the control torque inputs were active throughout much of the experiment and significantly affected the implementation of the CLF-based control method. As shown in Fig. 1, for the leg angle motor (top graph), the raw (desired) control torque was at times more than 400% of the (actually implemented) saturated value. Moreover, this occured over a significant duration

---

[3]See [1] for a description of the experiment and a reference to the online video.
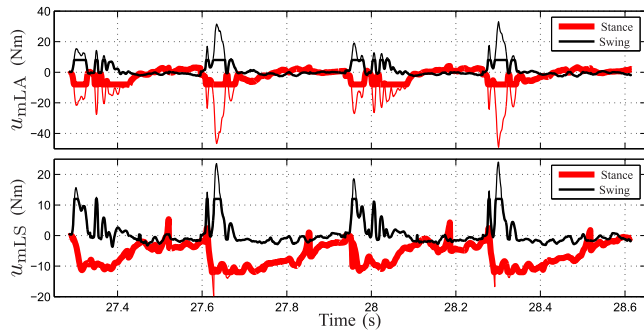
FIGURE 1. Motor torques (from the MABEL experiment described in [1]) for the stance and swing legs for 4 consecutive steps of walking with the minimum-norm CLF-based controller given in (19). The thicker plots indicate the experimental (saturated) torques, while the thinner plots are the raw (unsaturated) torques computed by the CLF-based controller. Note that the symbols u_{mLA}, u_{mLS} indicate the motor torques at the *leg angle* and *leg shape* coordinates respectively, which are linear combinations of the thigh and knee angles [18].

of the step. Though necessary to prevent unsafe or damaging motions, these saturation constraints were not applied in a manner that appropriately preserved the qualities of the CLF-based controller, and therefore the nominal bounds given by (14) and (17) were frequently violated.

Limits for control inputs are typically imposed by the user to ensure that motor torque specifications are not exceeded. When the calculated ideal control effort frequently exceeds the prescribed bounds and must therefore be truncated, the controller performance is degraded and theoretical performance measures may be violated, as in the experiment described above. More importantly, when a control input is saturated, the system runs in open-loop and is no longer able to respond to increasing errors in tracking, often leading to eventual failure.

Designing controllers which respect such bounds is important, and therefore a variety of approaches have been developed, such as quasi-linear control [16], which offers one solution for a special class of systems. In the specific context of input-output linearization, one approach is to attempt to map the actual input constraints for the original system to constraints on the corresponding control input for the linearized system.[4] The main objective of the current work is to present a method for implementing CLF-based controllers for a general class of nonlinear systems in a manner which respects the user-specified input bounds, making use of quadratic programming with relaxations.

IV. FORMULATING THE CLF MIN-NORM CONTROLLER AS A CONVEX OPTIMIZATION

To design such a controller, we proceed by recognizing that the pointwise min-norm controller in (19) can be equivalently expressed as a convex optimization problem formulated as

$$\min_{\mu} \mu^T \mu$$
$$\text{s.t.} \quad \psi_{0,\varepsilon}(\eta, z) + \psi_{1,\varepsilon}(\eta, z) \mu \leq 0. \quad (20)$$

[4]See [17], for instance, where input-output linearization is combined with linear model predictive control (LMPC) to implement such an approach.

The inequality constraint above enforces the bound on the time-derivative of the CLF given by (14), which can be equivalently expressed as $\dot{V}_\varepsilon(\eta) \leq -c_3/\varepsilon \, V_\varepsilon(\eta)$. The solution of this convex optimization problem is then exactly the controller specified in (19).

Remark 1: To clearly see that (20) is in fact equivalent to (19), note that for $\psi_{0,\varepsilon}(\eta, z) \leq 0$, the above optimization in (20) has the optimal solution $\mu^* = 0$. This is exactly the second case of (19). Next considering $\psi_{0,\varepsilon}(\eta, z) > 0$ and minimizing $\mu^T \mu$ subject to the equality constraint $\psi_{0,\varepsilon}(\eta, z) + \psi_{1,\varepsilon}(\eta, z)\mu = 0$, we have the analytical solution of the equality-constrained quadratic program through the Lagrange-dual method as exactly the first case of (19).

Once we have expressed the pointwise min-norm controller as a convex optimization problem, we can introduce bounds on the control input in the form of additional constraints for the convex optimization problem. However, for these potentially conflicting additional constraints to be satisfied, we first need to relax the bound on the time-derivative of the CLF. We do this by requiring $\dot{V}_\varepsilon(\eta) \leq -c_3/\varepsilon \, V_\varepsilon(\eta) + d_1$, for some $d_1 > 0$. The new optimization problem is formulated as

$$\min_{\mu, d_1} \mu^T \mu + p_1 d_1^2$$
$$\text{s.t.} \quad \psi_{0,\varepsilon}(\eta, z) + \psi_{1,\varepsilon}(\eta, z) \mu \leq d_1,$$
$$(L_g L_f y(q, \dot{q}))^{-1} \mu \geq (u_{min} - u^*),$$
$$(L_g L_f y(q, \dot{q}))^{-1} \mu \leq (u_{max} - u^*), \quad (21)$$

where p_1 is a large positive number that represents the penalty of relaxing the inequality constraints and u^* is defined by (5). The last two inequalities above are torque constraints and essentially enforce $u_{min} \leq u \leq u_{max}$ with u as defined in (7).

The formulation in (21) deals with the non-ideal context of saturated control inputs and therefore cannot ensure the same type of stability claims as those provided by [1, Th. 2], since relaxations in the bound on $\dot{V}_\varepsilon$ result in a loss of the RES-CLF quality for V_ε. However, given a prescribed convergence bound and a set of saturation constraints, the control described by (21) is guaranteed to perform at least as well as any other controller in the sense that it will keep V_ε in the smallest possible level set. In this sense, the CLF-based controller (21) can "match" the performance of any other controller in regards to bounding the growth of the RES-CLF V_ε. We also note that, though (21) as formulated does not guarantee Lipschitz continuity of the resultant controller, the work in [19] provides sufficient conditions to ensure Lipschitz continuity for these types of problems.

Remark 2: We note that (21) can also be formulated with "soft" bounds on the control inputs, such that the control input u in (7) satisfies $u_{min} - d_2 \leq u \leq u_{max} + d_3$, for some $d_2, d_3 > 0$. This alternative formulation provides the control designer with parameters to trade off violation of the bound on the time-derivative of the CLF with that of the saturation bound on the control input. However, in most practical cases the bounds on the inputs appear as hard bounds which cannot be relaxed, and the current work will focus only on this case.

Remark 3: Note that in (21) we have depicted u_{min} and u_{max} as constants. However, since the convex optimization problem is to be solved at every instant in time, these values can be specified as functions of time or system state, leading to *dynamic torque saturation*. For instance, the inequality constraint $u_{min}(t, q, \dot{q}) \le u \le u_{max}(t, q, \dot{q})$ can be specified with time and state-dependent dynamic bounds.

Remark 4: In Section II-B we presented an input-output linearizing controller based on PD control, given by (7) with (11). As formulated, the controller has no built-in means for dealing with saturation constraints, but we note that this controller can also be formulated as a convex optimization problem analogous to (21), as

$$\min_{u,d_1,d_2,d_3,d_4} u^T u + \sum_{i=1}^{4} p_i\, d_i^2$$
$$\text{s.t.} \quad L_g L_f h u = -L_f^2 h - \frac{K_P}{\varepsilon} h - \frac{K_D}{\varepsilon^2} L_f h$$
$$+ [d_1, \dots, d_4]^T,$$
$$u \ge u_{min},$$
$$u \le u_{max}, \quad (22)$$

where K_P and K_D are diagonal matrices satisfying the Hurwitz assumption of (12). However, unlike the CLF-based controller in (21), this formulation does not provide a clear correspondence between the relaxations d_i and performance of the controller. (Here we consider controller performance in terms of imposing a bound on $\dot{V}_\varepsilon$.) This highlights one of the main advantages of using the QP implementation of the CLF-based controller over the IO controller (either the original implementation or the QP version). Under active saturation constraints, the CLF-based controller relaxes the bound on $\dot{V}_\varepsilon$ just enough to balance the conflicting requirements between performance and saturation constraints. In contrast, the original IO controller ((7) with (11)) ''blindly'' saturates controls, and the QP version (22) relaxes an equality constraint in a manner that does not clearly correlate to the bound on $\dot{V}_\varepsilon$.

V. SIMULATION AND EXPERIMENTAL RESULTS

In this section we present both numerical simulation and experimental results to validate the performance of the control methods described in Section IV. MABEL is a planar bipedal robot comprised of five links that are assembled to form a torso and two legs with knees. The planar nature arises from the hips being constrained to revolve in the sagittal plane. The robot is attached to a boom and walks in a circle of a large radius so as to approximate locomotion in a straight line. MABEL has point feet and series-compliant actuation for improved agility and energy efficiency. The robot weighs 58 kg, is 1 m at the hip, and employs cable-differentials for connecting two motors to the hip and knee joints. This is done in such a way that one motor controls the angle of a virtual leg, consisting of the line connecting the hip to the toe, and the second motor is in series with a spring in order to control the length of the virtual leg. The experimental

setup has been described previously in [4] and is illustrated in Figure 7. MABEL has various sensors in the form of encoders for measuring various joint and pulley differential angles as well as contact sensors on the feet. Furthermore, sensors on the boom enable finding the planar position of the hip as well as the orientation of the torso with respect to the world frame. Numerical differentiation techniques are used to obtain low-noise and low-latency velocity estimates. Since experimental testing on MABEL was the ultimate goal, the numerical studies were conducted first on a simple model of MABEL, followed by simulations on a complex model of MABEL developed in [18], which closely replicates the experimental setup. This latter model includes a compliant ground model as well as a model that allows for stretch in the cables between the transmission pulleys. For the simulations and experiments described here, the four output functions were defined by the absolute pitch angle of the torso, the leg angle (LA) for the swing leg, and the appropriately scaled leg-shape motor position (mLS) for the swing and stance legs. The four control inputs are the leg-angle motor torque ($u_{mLA_{st}}, u_{mLA_{sw}}$) and leg-shape motor torque ($u_{mLS_{st}}, u_{mLS_{sw}}$) for the stance and swing legs respectively.

A. NUMERICAL SIMULATION
#### 1) CLF-QP CONTROLLER UNDER VARIOUS TORQUE BOUNDS
The numerical simulation results presented here employ the CLF-based controller with hard input constraints, as in (21). We consider four separate cases with different control bounds, given by,

$$A: \left\{ \begin{bmatrix} -8 \\ -12 \\ -8 \\ -12 \end{bmatrix} \le \begin{bmatrix} u_{mLA_{st}} \\ u_{mLS_{st}} \\ u_{mLA_{sw}} \\ u_{mLS_{sw}} \end{bmatrix} \le \begin{bmatrix} 8 \\ 12 \\ 8 \\ 12 \end{bmatrix} \right.,$$

$$B: \left\{ \begin{bmatrix} -5 \\ -8 \\ -2 \\ -2 \end{bmatrix} \le \begin{bmatrix} u_{mLA_{st}} \\ u_{mLS_{st}} \\ u_{mLA_{sw}} \\ u_{mLS_{sw}} \end{bmatrix} \le \begin{bmatrix} 4 \\ 4 \\ 4 \\ 4 \end{bmatrix} \right.,$$

$$C: \left\{ \begin{bmatrix} -4 \\ -8 \\ -2 \\ -2 \end{bmatrix} \le \begin{bmatrix} u_{mLA_{st}} \\ u_{mLS_{st}} \\ u_{mLA_{sw}} \\ u_{mLS_{sw}} \end{bmatrix} \le \begin{bmatrix} 1 \\ 1 \\ 1 \\ 1 \end{bmatrix} \right.,$$

$$D: \left\{ \begin{bmatrix} -4 \\ -6 \\ -2 \\ -2 \end{bmatrix} \le \begin{bmatrix} u_{mLA_{st}} \\ u_{mLS_{st}} \\ u_{mLA_{sw}} \\ u_{mLS_{sw}} \end{bmatrix} \le \begin{bmatrix} 1 \\ 1 \\ 1 \\ 1 \end{bmatrix} \right.,$$

where the input bounds get more stringent as we progress from Case A to Case D.

Simulations of a representative walking step with the controller (21) were run for each of Cases A-D; the corresponding RES-CLF V_ε and its time derivative are

presented in Figure 2. In all the simulations, the same initial perturbation off of the periodic orbit was provided; in particular, both joint angles and velocities were perturbed from their nominal values. (For instance, the torso was perturbed to lean backward by an additional 3° from the nominal.) As can be seen, for the stringent saturation in Case D, the time derivative of the Lyapunov function violates the bound in (14) and moreover actually becomes positive with a large value for a part of the gait. Nonetheless, the controller is still able to drive the errors to zero by the end of the gait. The resulting input torques and tracking errors are illustrated in Figure 3. The saturation effects are most visible in the plots in the first and third rows of the figure; as expected, more restrictive torque limits result in increased tracking error. However, we observe that the degradation in performance is gradual and walking stability is still maintained for all cases (A-D) of input saturation.
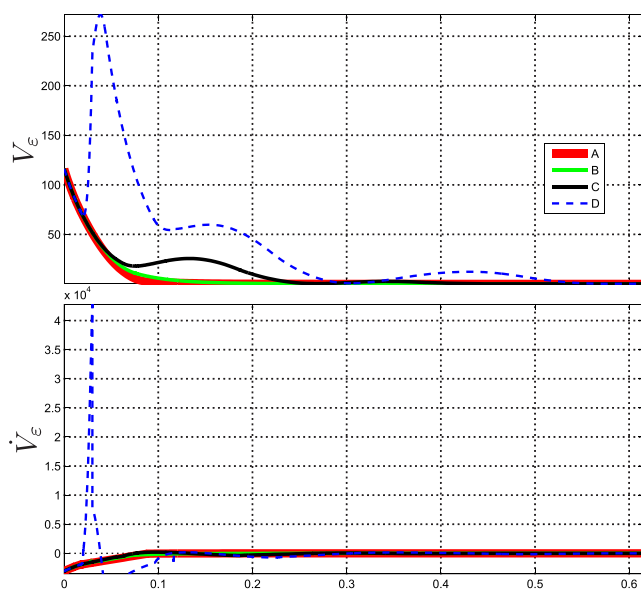
FIGURE 2. The RES-CLF V_ε and its derivative under the CLF-QP controller (21) for the numerical simulations described in the first part of Section V-A. The figures depict the results for the same initial perturbation off of the periodic orbit with four increasingly stringent torque bounds.

Remark 5: It should be noted that successful walking depends on parameter choices, and there are circumstances under which the proposed controller does fail. For instance, stringent saturation for $u_{\mathrm{mLS}_{st}}$ (corresponding to the stance knee) can result in failure, since a minimum torque is required to hold up the weight of the robot and prevent the stance knee from buckling. For the case where errors at the start of the gait are significantly larger than those depicted in Figure 2 (i.e. initial value of V_ε is larger), stringent saturations such as those in Case D will lead to instability within a few steps.

To illustrate the effect of saturation on the walking limit cycle, we also carry out simulations on the complex model of MABEL. We use the controller given by (21) in closed-loop and analyze the phase portrait of the torso angle, subject to

several different saturation values. Figure 4 illustrates the torso phase portrait for 15 steps of walking, and we observe that stricter saturations result in (gradual) deterioration in tracking, as evidenced by deviations of the limit cycle from the nominal orbit. The saturation values used here differ from those used in the simulations described in the first part of this section, since the complex model differs significantly from the simple model and the required torques for walking are different, but the approach is analogous, with bounds becoming increasingly restrictive proceeding from Case I to Case IV. More specifically, Case I corresponds to $-8 \leq u_{\mathrm{mLA}} \leq 8$, $-12 \leq u_{\mathrm{mLS}} \leq 12$, Case II corresponds to $-6 \leq u_{\mathrm{mLA}} \leq 4$, $-6.5 \leq u_{\mathrm{mLS}} \leq 4$, Case III corresponds to $-4 \leq u_{\mathrm{mLA}} \leq 2$, $-6 \leq u_{\mathrm{mLA}} \leq 3$, and Case IV corresponds to a dynamic torque bound that is a function of the state of the robot.

2) COMPARISON OF CLF-BASED CONTROLLER WITH IO-LINEARIZING PD CONTROL

Having demonstrated that the CLF-QP controller is capable of functioning, albeit at degraded performance, under various levels of torque bounds, we will now attempt to compare the four controllers presented in this paper. In this section the controllers are termed as (a) *IO controller* referring to the input-output linearizing controller, (7) with (11); (b) *CLF controller* referring to the CLF-based min-norm controller, (19); (c) *CLF-QP controller* referring to the CLF-based min-norm controller posed as a quadratic program with additional input constraints, (21); and (d) *IO-QP controller* referring to the input-output controller posed as a quadratic program along with the additional input bound constraints, (22). For each of these controllers, one step of walking is simulated with an initial error and with the restrictive input saturation constraints of case C.

It must be noted that direct comparison of the performance of the CLF controller and IO controllers is difficult and somewhat anecdotal because of the heavy dependance on parameter tuning. We note that for the CLF-QP controller, performance depends on

- selection of the RES-CLF V_ε,
- the relaxation penalty p_1,
- and the parameter ε which dictates the bound on $\dot{V}_\varepsilon$,

while the IO controller is dependent on the selection of ε and the parameters K_P and K_D. For this comparison, we use the same ε for all controllers, however the relaxation penalty for the CLF controller and the PD gains for the IO controller are selected separately. A study of best procedures for tuning the CLF controller and for comparison of controller performance is not the subject of the current work, but presents an interesting field of study for future research.

The controllers are compared in Table 1, and graphical results of numerical simulations are presented in Figures 5-6. In the particular simulations at hand, Table 1 illustrates that under the same conditions, the CLF-QP controller spends the least amount of time having one or more actuators in saturation and also results in the most energy efficient gait, as computed by the specific cost of mechanical transport [20].
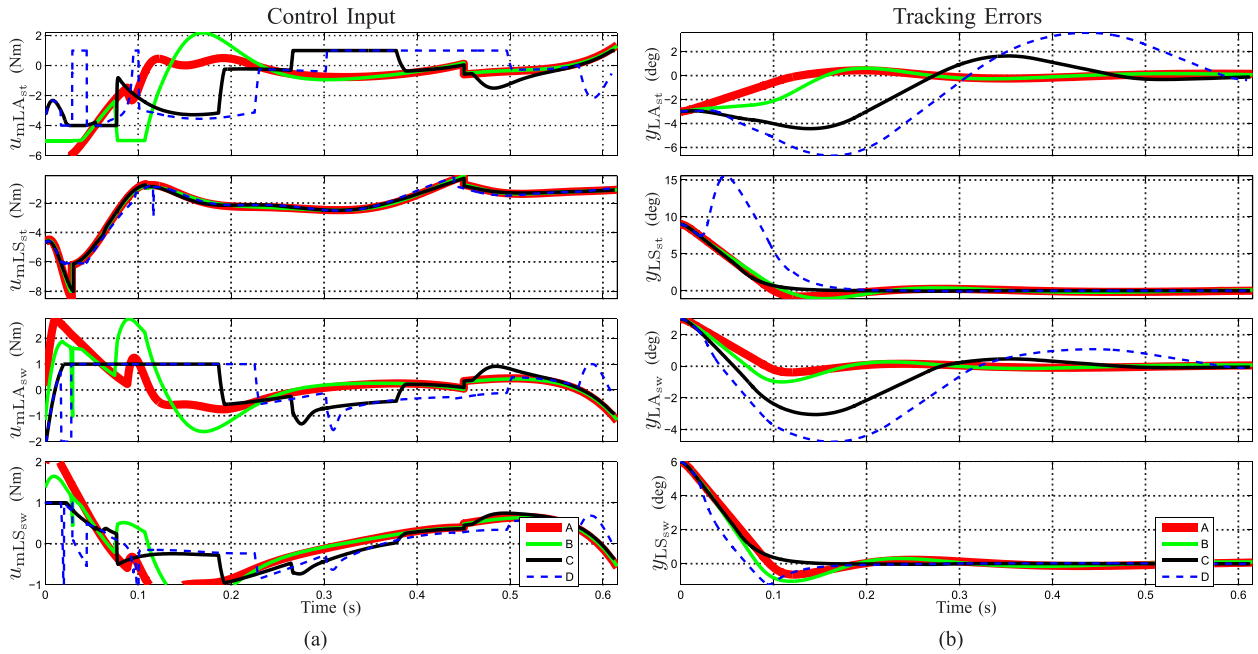
FIGURE 3. Motor torque plots obtained by simulating the proposed CLF-QP controller with four different cases of torque saturation. (a) Motor torques for the stance (top two figures) and swing legs (bottom two figures), and (b) Corresponding errors in tracking the output *y*(*q*), based on the numerical simulations described in Section V-A. Each figure depicts the results for four different cases of input bounds. Walking stability is maintained in each case, but we note that the stringent torque bounds in Case C result in control inputs that are only piece-wise continuous. For obtaining Lipschitz continuous control inputs, see additional required conditions in [19].
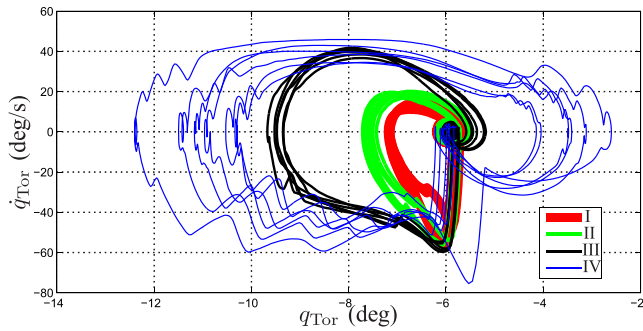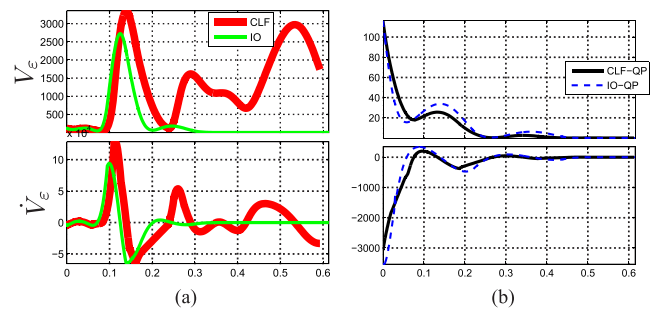

FIGURE 4. Phase portrait of the torso angle for four different cases of input bounds, as described in Section V-A. Observe that stricter saturations result in (gradual) deterioration in tracking, as evidenced by deviations of the limit cycle from the nominal orbit.

FIGURE 5. The RES-CLF V_ε and its derivative under (a) the CLF and IO controllers and (b) the CLF-QP and IO-QP controllers, as described in the second part of Section Section V-A.

TABLE 1. Comparison between the different types of controllers presented in this paper when under hard input saturation. The second column represents the percentage of time for which one or more actuators are in saturation, and the third column presents the specific cost of mechanical transport. The results are suggestive that CLF-QP may be the most efficient of the four controllers, with less time in saturation likely resulting in lower cost of mechanical transport, but additional investigation is required to further explore the comparison.

Controller	% Time in Saturation	C_{mt}
IO (7), (11)	68%	0.021
CLF (19)	91%	0.092
CLF-QP (21)	23%	0.008
IO-QP (22)	65%	0.016

However, as noted previously, comparison of controller performance is somewhat anecdotal due to the reliance on parameter tuning and thus the results in Table 1 should be

viewed accordingly. The comparison does suggest that the (non-QP) CLF controller performs the worst under input saturations since the controller has no awareness of saturation constraints, and thus even when the actuators are not in saturation the controller does not act aggressively to reduce the large errors that have built up. Figure 5 illustrates the RES-CLF V_ε and its time-derivative for all the controllers. For the two controllers which do not incorporate knowlege of the input saturations (i.e. the CLF and IO controller), V_ε grows considerably, although the IO controller is able to quickly decrease the errors once the calculated control torques are within saturation limits. Figure 6b illustrates the tracking errors for the controllers. Note that the CLF controller is unable to control the growing errors and results in instability under these stringent torque bounds.
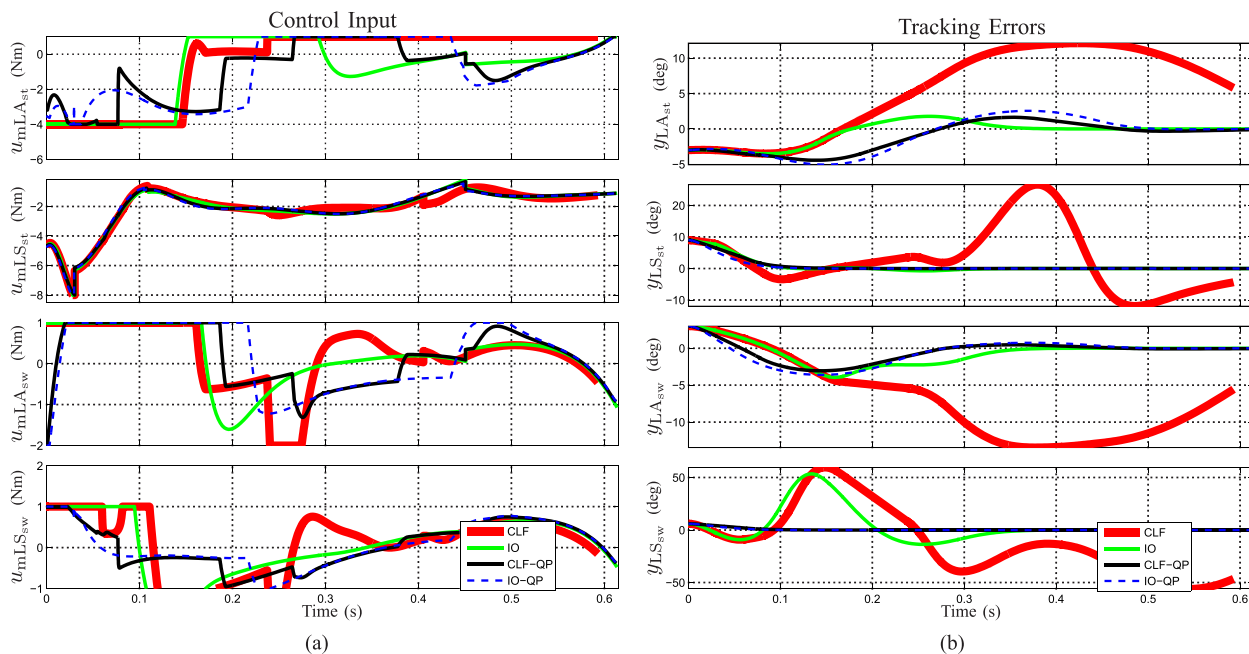
FIGURE 6. Motor torque plots obtained by simulating four different controllers with the same torque saturation. (a) Motor torques for the stance (top two figures) and swing legs (bottom two figures), and (b) Corresponding errors in tracking the output $y(q)$, based on the numerical simulations described in Section V-A. Each figure depicts the results for the four controllers presented in this paper with hard input saturation. Only the CLF controller leads to instability, while the IO, IO-QP and CLF-QP controllers stabilize to the periodic walking gait. Note that this plot is not intended to serve as a decisive comparison of the tracking capabilities of the CLF-QP vs. the IO-QP controller (which will require further analysis), but does demonstrate that CLF-QP tracking performance surpasses the simple CLF controller and is qualitatively similar to IO-QP.
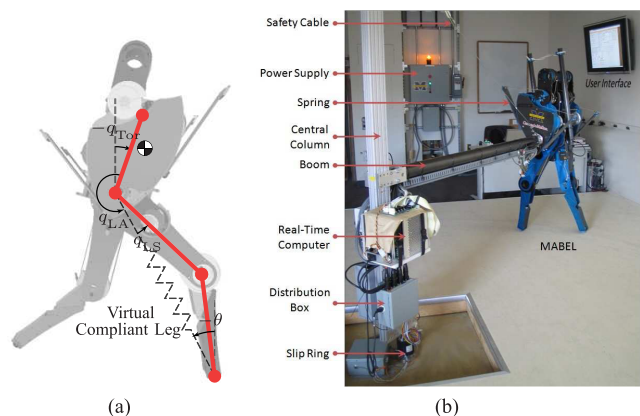
FIGURE 7. Experimental setup for bipedal robot MABEL and associated coordinates. (From [4].) (a) Coordinates. (b) MABEL experimental setup.

B. EXPERIMENTAL RESULTS

Motivated by the favorable numerical simulation results, we proceed to test the controller experimentally on MABEL. Experimental implementation of the CLF controller at real-time speeds is a challenging task, since it requires computation of the system dynamics (2), the Lie derivatives of the output $y(q)$, and the CLF controller terms (18), as well as the solving of a convex optimization problem. In order to meet hard real-time constraints of 1 kHz, these computations must be completed in less than 1 ms. By employing the custom-code generation method CVXGEN [21] for solving

constrained quadratic programs, we are able to solve the optimization problem in a few hundred microseconds and meet the 1 kHz update requirement, making experimental implementation feasible.

In this experiment, we implemented the CLF controller described in (21), with the CLF-bound penalty set at $p_1 = 50$ and with torque bounds u_{min}, u_{max} chosen such that $-8 \leq u_{mLA} \leq 8$, $-12 \leq u_{mLS} \leq 12$. This experiment resulted in 70 steps of walking for MABEL and is portrayed in the video in [22]. (A photo sequence depicting one representative step is also shown in Figure 8.) Figure 9 illustrates the resultant control torques; we observe that the user-specified control bounds are respected, as evidenced by the flattened control signals at the boundary areas. Note that the green squares on the plot depict the time instances at which control bounds are not met, which occur at moments in which the convex optimization algorithm is not able to converge within the specified time constraints. These occurrences are isolated


FIGURE 8. A photo sequence depicting one representative step from the experiment described in Section V-B.
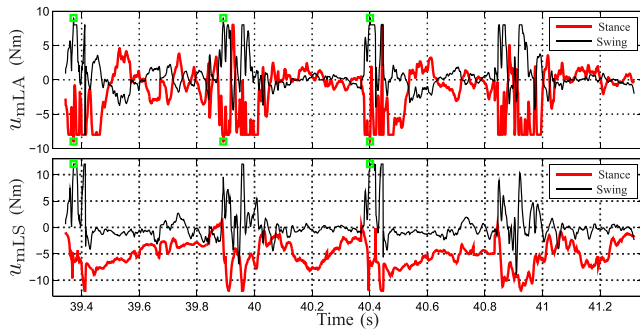
FIGURE 9. Motor torques (from the walking experiment with MABEL) for the stance and swing legs for 4 consecutive steps of walking with the CLF controller with convex optimization and strict torque limits (8 Nm in the top graph and 12 Nm in the bottom). The green square markers on the plots indicate isolated time instances at which the user-specified torque bound was exceeded by the convex optimization due to hard real-time constraints for experimental implementation.
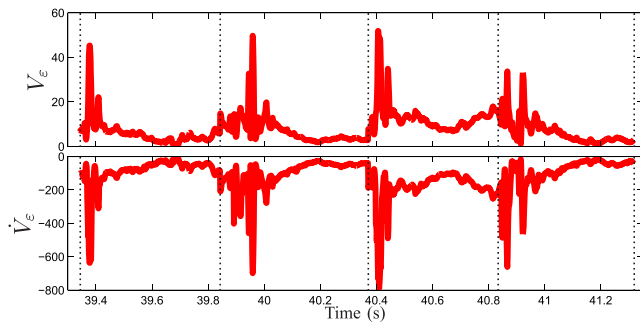
FIGURE 10. The RES-CLF V_ε and its time-derivative (from the walking experiment with MABEL) for 4 consecutive steps of walking with the CLF controller with convex optimization and strict torque limits. Note that the time derivative of V_ε is computed from the experimental data on the best model of the system we have. There are instance in this plot when $\dot{V}_\varepsilon$ is negative while V_ε is increasing, which is most likely due to model uncertainty.

and have no affect on the experimental system since a motor is not able to respond to them. Figure 10 illustrates the Lyapunov function V_ε and its time derivative for this experiment. The fact that the Lypanuov function V_ε increases at some points where the calculated $\dot{V}_\varepsilon$ is negative is most likely due to model uncertainty, since $\dot{V}_\varepsilon$ is calculated (online) along trajectories of the partially linearized system (8) and depends upon the model dynamics through the pre-control (7).

VI. CONCLUSION
We have presented a novel method that explicitly addresses input saturation in the feedback control design for achieving walking in bipedal robots. The resulting controller enables gradual performance degradation while still continuing to walk under a range of stringent torque limits. We accomplish this through an alternative method for implementing the pointwise min-norm CLF-based controller described in (19) in a manner that more appropriately handles input saturations. Numerical simulation as well as experimental implementation has demonstrated that these control methods

can be very useful in practice, even in systems which require a high real-time control update rate. This method has great potential for effectively dealing with saturations in a variety of contexts, such as power-limited systems which could progressively lower user-defined torque saturations as the battery charge decreases, thereby prolonging the last bit of battery charge while allowing system performance to gracefully degrade. In addition to dynamic torque saturation, we also note that this approach provides a method for incorporating a whole family of user-defined constraints into the online calculation of controller effort for the types of systems described here. For example, the work described in [23] extends the results of this paper to show how the CLF QP control scheme can be used to unify locomotion, manipulation, and force-based tasks in a holistic fashion. Future work will consider the effects of varying ε throughout the gait, which may result in an improved trade-off between convergence rate and saturation response over the course of the step.

REFERENCES
[1] A. D. Ames, K. Galloway, J. W. Grizzle, and K. Sreenath, "Rapidly exponentially stabilizing control Lyapunov functions and hybrid zero dynamics," *IEEE Trans. Autom. Control*, vol. 59, no. 4, pp. 876–891, Apr. 2014.
[2] E. R. Westervelt, J. W. Grizzle, and D. E. Koditschek, "Hybrid zero dynamics of planar biped walkers," *IEEE Trans. Autom. Control*, vol. 48, no. 1, pp. 42–56, Jan. 2003.
[3] E. R. Westervelt, J. W. Grizzle, C. Chevallereau, J.-H. Choi, and B. Morris, *Feedback Control of Dynamic Bipedal Robot Locomotion*. Boca Raton, FL, USA: CRC Press, 2007.
[4] K. Sreenath, H.-W. Park, I. Poulakakis, and J. W. Grizzle, "A compliant hybrid zero dynamics controller for stable, efficient and fast bipedal walking on MABEL," *Int. J. Robot. Res.*, vol. 30, no. 9, pp. 1170–1193, Aug. 2011.
[5] D. S. Bernstein and A. N. Michel, "A chronological bibliography on saturating actuators," *Int. J. Robust Nonlinear Control*, vol. 5, no. 5, pp. 375–380, 1995.
[6] M. Hardt, K. Kreutz-Delgado, and J. W. Helton, "Optimal biped walking with a complete dynamical model," in *Proc. 38th IEEE Conf. Decision Control*, Dec. 1999, pp. 2999–3004.
[7] M. W. Spong, J. S. Thorp, and J. M. Kleinwaks, "The control of robot manipulators with bounded input," *IEEE Trans. Autom. Control*, vol. AC-31, no. 6, pp. 483–490, Jun. 1986.
[8] C. Chevallereau, A. Formal'sky, and B. Perrin, "Low energy cost reference trajectories for a biped robot," in *Proc. IEEE Int. Conf. Robot. Autom.*, May 1998, pp. 1398–1404.
[9] Y. Wang and S. Boyd, "Fast evaluation of quadratic control-Lyapunov policy," *IEEE Trans. Control Syst. Technol.*, vol. 19, no. 4, pp. 939–946, Jul. 2011.
[10] D. J. Braun and M. Goldfarb, "A control approach for actuated dynamic walking in biped robots," *IEEE Trans. Robot.*, vol. 25, no. 6, pp. 1292–1303, Dec. 2009.
[11] T. Sugihara and Y. Nakamura, "Whole-body cooperative balancing of humanoid robot using COG Jacobian," in *Proc. IEEE/RSJ Int. Conf. Intell. Robots Syst.*, vol. 3. Oct. 2002, pp. 2575–2580.
[12] P.-B. Wieber, "Trajectory free linear model predictive control for stable walking in the presence of strong perturbations," in *Proc. 6th IEEE-RAS Int. Conf. Humanoid Robots*, Dec. 2006, pp. 137–142.
[13] D. Dimitrov, A. Sherikov, and P.-B. Wieber, "A sparse model predictive control formulation for walking motion generation," in *Proc. IEEE Int. Conf. Intell. Robots Syst.*, Sep. 2011, pp. 2292–2299.
[14] A. Isidori, *Nonlinear Control Systems: An Introduction*, 2nd ed. Berlin, Germany: Springer-Verlag, 1989.
[15] R. A. Freeman and P. V. Kokotović, *Robust Nonlinear Control Design*. Boston, MA, USA: Birkhäuser, 1996.

[16] S. Ching, Y. Eun, C. Gokcek, P. T. Kabamba, and S. M. Meerkov, *Quasilinear Control: Performance Analysis and Design of Feedback Systems With Nonlinear Sensors and Actuators*. Cambridge, U.K.: Cambridge Univ. Press, 2011.

[17] M. J. Kurtz and M. A. Henson, "Input-output linearizing control of constrained nonlinear processes," *J. Process Control*, vol. 7, no. 1, pp. 3–17, Feb. 1997.

[18] H.-W. Park, K. Sreenath, J. W. Hurst, and J. W. Grizzle, "Identification of a bipedal robot with a compliant drivetrain," *IEEE Control Syst.*, vol. 31, no. 2, pp. 63–88, Apr. 2011.

[19] B. Morris, M. J. Powell, and A. D. Ames, "Sufficient conditions for the Lipschitz continuity of QP-based multi-objective control of humanoid robots," in *Proc. 52nd IEEE Conf. Decision Control*, Dec. 2013, pp. 2920–2926.

[20] S. Collins, A. Ruina, R. Tedrake, and M. Wisse, "Efficient bipedal robots based on passive-dynamic walkers," *Science*, vol. 307, no. 5712, pp. 1082–1085, 2005.

[21] J. Mattingley and S. Boyd, "CVXGEN: A code generator for embedded convex optimization," *Optim. Eng.*, vol. 13, no. 1, pp. 1–27, Mar. 2012.

[22] K. Galloway, K. Sreenath, A. Ames, and J. Grizzle. (2013). *Walking With CLF Control + Dynamic Torque Saturation*, Youtube Video. [Online]. Available: http://youtu.be/rc1FSXpfrrM

[23] A. D. Ames and M. Powell, "Towards the unification of locomotion and manipulation through control Lyapunov functions and quadratic programs," in *Control of Cyber-Physical Systems* (Lecture Notes in Control and Information Sciences), vol. 449, D. C. Tarraf, Ed. Berlin, Germany: Springer-Verlag, 2013, pp. 219–240.

KOUSHIL SREENATH received the B.E. degree in electronics and communications from the Vishveshwarya Technological University, India, in 2002, the M.S. degree in Electrical Engineering from the University of Texas at Arlington, TX, in 2005, and the M.S. degree in applied mathematics and Ph.D. degree in electrical engineering: systems from the University of Michigan at Ann Arbor, MI, in 2011, respectively. His work on dynamic legged locomotion on the bipedal robot MABEL was featured on The Discovery Channel, CNN, ESPN, FOX, and CBS. His work on dynamic aerial manipulation was featured on the IEEE Spectrum, New Scientist, and Huffington Post. He is currently an Assistant Professor of Mechanical Engineering and a Courtesy Assistant Professor with the Robotics Institute, and Electrical and Computer Engineering, Carnegie Mellon University. His research interest lies at the intersection of highly dynamic robotics and applied nonlinear control. His work on adaptive sampling with mobile sensor networks was published as a book entitled *Adaptive Sampling with Mobile WSN* (IET). He received the best paper award at the Robotics: Science and Systems Conference in 2013, and the Google Faculty Research Award in Robotics in 2015.

AARON D. AMES received the B.S. degree in mechanical engineering and the B.A. degree in mathematics from the University of St. Thomas, in 2001, and the M.A. degree in mathematics and the Ph.D. degree in electrical engineering and computer sciences from the University of California at Berkeley (UC Berkeley), in 2006. He served as a Post-Doctoral Scholar in Control and Dynamical Systems with the California Institute of Technology from 2006 to 2008. He is currently an Associate Professor and a Morris E. Foster Faculty Fellow II in Mechanical Engineering with Texas A&M University, with joint appointments in Electrical and Computer Engineering and Computer Science and Engineering. His research interests center on robotics, nonlinear control, hybrid systems, and cyber-physical systems, with a special emphasis on foundational theory and experimental realization on bipedal robots. At UC Berkeley, he was a recipient of the 2005 Leon O. Chua Award for his achievement in nonlinear science and the 2006 Bernard Friedman Memorial Prize in Applied Mathematics. He received the NSF CAREER Award for his research on bipedal robotic walking and its applications to prosthetic devices in 2010.

KEVIN GALLOWAY received the B.S. degree in systems engineering from the United States Naval Academy, Annapolis, MD, in 1997, and the Ph.D. degree in electrical engineering from the University of Maryland, College Park, in 2011. From 2011 to 2013, he served as a Post-Doctoral Research Fellow with the Department of Electrical Engineering and Computer Science, University of Michigan, Ann Arbor, where he developed control methodology for robotic bipeds. He is currently an Assistant Professor with the Electrical and Computer Engineering Department, United States Naval Academy. His research interests focus on coordinated control of nonlinear systems, and include collective control of autonomous mobile agents and robotic-legged locomotion. He was a recipient of the L-3 Graduate Research Fellowship from the University of Maryland.

JESSY W. GRIZZLE (F'97) received the Ph.D. degree in electrical engineering from The University of Texas at Austin, in 1983. He held an NSF-NATO Post-Doctoral Fellowship in Science in Paris, France, in 1984. Since 1987, he has been with the University of Michigan, Ann Arbor, where he is currently the Jerry and Carol Levin Professor of Engineering and the Elmer Gilbert Distinguished University Professor. His work on bipedal locomotion has been the object of numerous plenary lectures, and has been featured in *The Economist*, *Wired Magazine*, *Discover Magazine*, *Scientific American*, *Popular Mechanics*, and several television programs. He jointly holds 16 patents dealing with emissions reduction in passenger vehicles through improved control system design. He is a fellow of the International Federation of Automatic Control. He was a recipient of the Paper of the Year Award from the IEEE Vehicular Technology Society in 1993, the George S. Axelby Award in 2002, the Control Systems Technology Award in 2003, and the Bode Lecture in 2012.

• • •